



Air pollution increases human health risks of PM_{2.5}-bound PAHs and nitro-PAHs in the Yangtze River Delta, China



Youwei Hong^{a,b,c,d}, Xinbei Xu^{a,b,c}, Dan Liao^e, Xiaoting Ji^{a,b,c}, Zhenyu Hong^{a,b}, Yanting Chen^{a,b}, Lingling Xu^{a,b}, Mengren Li^{a,b}, Hong Wang^g, Han Zhang^{a,b}, Hang Xiao^{a,b}, Sung-Deuk Choi^f, Jinsheng Chen^{a,b,*}

^a Center for Excellence in Regional Atmospheric Environment, Institute of Urban Environment, Chinese Academy of Sciences, Xiamen 361021, China

^b Key Lab of Urban Environment and Health, Institute of Urban Environment, Chinese Academy of Sciences, Xiamen 361021, China

^c University of Chinese Academy of Sciences, Beijing 100049, China

^d College of Resources and Environment, Fujian Agriculture and Forest University, Fuzhou 350002, China

^e College of Environment and Public Health, Xiamen Huaxia University, Xiamen 361024, China

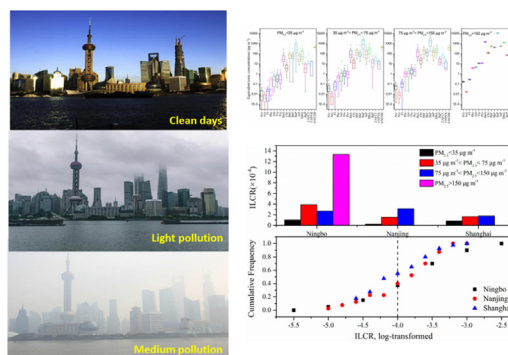
^f Department of Urban and Environmental Engineering, Ulsan National Institute of Science and Technology, Ulsan 44919, South Korea

^g Fujian Meteorological Science Institute, Fujian Key Laboratory of Severe Weather, Fuzhou 350001, China

HIGHLIGHTS

- Sources and risks of PM_{2.5}-bound PAHs and NPAHs in the YRD region of China were investigated.
- Different PM_{2.5} pollution levels change the occurrence and fate of PAHs and NPAHs.
- Typical NPAH analysis indicated contribution of secondary formation via photochemical reaction.
- Human health risks of PAHs and NPAHs during haze days were sharply enhanced.

GRAPHICAL ABSTRACT



ARTICLE INFO

Article history:

Received 11 November 2020

Received in revised form 20 January 2021

Accepted 20 January 2021

Available online 27 January 2021

Editor: Jay Gan

Keywords:

PAHs
NPAHs
PM_{2.5}
Health risk
The Yangtze River Delta

ABSTRACT

Identifying the nature and extent of atmospheric PM_{2.5}-bound toxic organic pollutants is beneficial to evaluate human health risks of air pollution. Seasonal observations of PM_{2.5}-bound polycyclic aromatic hydrocarbons (PAHs) and nitro-PAHs (NPAHs) in the Yangtze River Delta (YRD) were investigated, along with criteria air pollutants and meteorological parameters. With the elevated PM_{2.5} level, the percentage of 4-ring PAHs and typical NPAH including 3-Nitrobiphenyl (3-NBP) and 2-Nitrofluoranthene (2-NFLT) increased by 19–40%. PM_{2.5}-bound 2-NFLT was positively correlated with O₃ and NO₂, suggesting the contribution of atmospheric oxidation capacity to enhance the secondary formation of NPAHs in the atmosphere. Positive matrix factorization (PMF) analysis indicated that traffic emissions (44.9–48.7%), coal and biomass combustion (27.6–36.0%) and natural gas volatilization (15.3–27.5%) were major sources of PAHs, and secondary formation (39.8–53.8%) was a predominant contributor to total NPAH concentrations. Backward trajectory analysis showed that air masses from North China transported to the YRD region increased PAH and NPAH concentrations. Compare to clean days, the BaP equivalent concentrations of total PAHs and NPAHs during haze pollution days were enhanced by 10–25 and 2–6 times, respectively. The Incremental Lifetime Cancer Risks (ILCRs) of PAHs by inhalation exposure also indicated high potential health risks in the YRD region. The results implied that the health risks of PM_{2.5}-bound PAHs and NPAHs could be sharply enhanced with the increase of PM_{2.5} concentrations.

© 2021 Elsevier B.V. All rights reserved.

* Corresponding author at: Institute of Urban Environment, Chinese Academy of Sciences, 1799 Jimei Road, Xiamen 361021, China.
E-mail address: jschen@iue.ac.cn (J. Chen).

1. Introduction

Air pollution due to fine particulates (PM_{2.5}) is globally increasing the relative risk of mortality from cerebrovascular disease, lung cancers, and chronic respiratory diseases (Cohen et al., 2017; Oliveira et al., 2019; Yin et al., 2020). Severe and persistent haze events frequently occurred in the megacities of developing countries, with daily concentrations of PM_{2.5} exceeding several hundred micrograms per cubic meter (Chen et al., 2020a, 2020b; Cheng et al., 2016; Huang et al., 2014). However, an emerging challenge is to understand the relationship between active components of PM_{2.5} and human health, including chemical toxicity, oxidative potential and bacteria, fungi, viruses, antibiotic resistance genes, pollens, and cell debris (Guan et al., 2016; Idowu et al., 2019; Xie et al., 2019).

In general, the toxicity of PM_{2.5} is partly originated from its chemical components (Lin et al., 2019; Yin et al., 2020). Many studies had found that polycyclic aromatic hydrocarbons (PAHs) could be an essential toxic component of PM_{2.5} (Hong et al., 2015; Lin et al., 2015; Yang et al., 2017). With the increase of atmospheric oxidizing capacity, more derivatives of PAHs such as nitrated PAHs (NPAHs) in PM_{2.5} were detected, probably resulting in high potential human health risks (Zhang et al., 2020).

In the atmosphere, PAHs mainly originated from anthropogenic activities such as incomplete burning of fossil fuels and biomass, partitioned between gaseous and particulate phases (Xu et al., 2006; Hong et al., 2015). NPAHs are mainly produced from chemical reactions of PAHs, and also from direct emissions of fuel combustions (Albinet et al., 2008; Bandowe and Meusel, 2017). Current studies suggested that large amounts of PM_{2.5}-bound NPAHs are formed via gas-phase reactions of semi-volatile PAHs and are gradually deposited on airborne particles (Lin et al., 2015; Tomaz et al., 2016; Wei et al., 2015). Compared with PAHs, little information on the source identification of PM_{2.5}-bound NPAHs was available, especially the relative contribution of these sources (Bandowe and Meusel, 2017; Ringuet et al., 2012). In addition, other air pollutants (e.g., ozone and particulate matter), meteorological conditions (e.g., temperature and humidity), and long-range transport could also affect the distribution and transformation of atmospheric PAHs and NPAHs, including gas-particle partitioning (Hu et al., 2019; Ma et al., 2020; Tomaz et al., 2016). There is a need to investigate the nature and extent of atmospheric PM_{2.5}-bound PAHs and NPAHs during rapid urbanization and to provide effective information for risk management strategies.

The Yangtze River Delta (YRD) is one of the most developed regions of China, which approximately accounts for 20% of the total GDP in China (Wang et al., 2016). In recent years, severe haze occurred more frequently in the YRD region (Li et al., 2019a). Most studies focused on the formation mechanism of secondary inorganic components and sources of PM_{2.5} in this region (Chen et al., 2020a, 2020b; Huang et al., 2014). However, there is limited information about pollution characteristics and their health risks of PM_{2.5}-bound PAHs and NPAHs under different PM_{2.5} pollution levels (He et al., 2014; Liu et al., 2018). In this study, PM_{2.5} samples in three cities of the YRD region were simultaneously collected during one whole year period. Seasonal and spatial distributions of PM_{2.5}-bound PAHs and NPAHs with different PM_{2.5} pollution levels were analyzed. Potential sources were identified by diagnostic parameters and positive matrix factorization (PMF) analysis. Backward trajectory analysis was also performed to evaluate the influences of local and regional sources in the YRD region. Combined with BaP equivalent concentrations, incremental lifetime cancer risks of PM_{2.5}-bound PAHs and NPAHs at a regional scale during severe air pollution periods were determined.

2. Materials and methods

2.1. Study area

Three cities in the YRD region, including Shanghai (SH), Nanjing (NJ) and Ningbo (NB), were selected to characterize pollution level, source

apportionment, and cancer risk assessment of PM_{2.5}-bound PAHs and NPAHs (Fig. S1). The sampling sites in SH and NJ were located at the Shanghai Academy of Environmental Science (SAES) and Nanjing University (Gulou District), respectively, which are close to commercial and residential areas. The monitoring site in NB was located at the University of Nottingham, and surrounded by teaching buildings. All the samplers were installed on the rooftop of the building, with a height of 18–21 m above the ground.

Online hourly mass concentrations of particulate matters (PM_{2.5} and PM₁₀) were measured using a tapered element oscillating microbalance (TEOM1405, Thermo Scientific Corp., MA, US) (Table S1). NO₂, SO₂, and O₃ were obtained using online analyzers (TEI 42i, 43i and 49i, Thermo Scientific Corp., MA, US). Ambient meteorological parameters including temperature (T), relative humidity (RH), wind speed (WS) and wind direction (WD) were monitored by an ultrasonic anemometer (150WX, Airmar, the USA). The maintenance/accuracy of all online instruments was validated according to our previous studies (Du et al., 2017).

2.2. Samples collection

A total of 120 samples and 24 field blanks in three cities were simultaneously collected during autumn (November 2014), winter (December 2014 to January 2015), spring (April 2015), and summer (July and August 2015). The 23-hour PM_{2.5} samples were collected on preheated (500 °C, 4 h) quartz microfiber filters (Whatman QMA, 203 mm × 254 mm) using a high-volume sampler (TH-1000H, Wuhan Tianhong Instruments Co., Ltd., China) at a flow rate of 1.05 m³ min⁻¹. The samples were covered with aluminum foil and stored at -20 °C until analysis.

2.3. PAHs and NPAHs analysis

According to our previous method (Hong et al., 2015), half of each quartz microfiber filter was cut into pieces and extracted using an accelerated solvent extraction system (ASE, Dionex 350) with dichloromethane (DCM)/methanol (2:1, V/V). All samples were weighed and placed in ASE extraction cells, spiked with 5 deuterated-PAHs (naphthalene-d₈, acenaphthene-d₁₀, phenanthrene-d₁₀, chrysene-d₁₂, and perylene-d₁₂) and deuterated-NPAH (3-nitrofluoranthene-d₉) as surrogate standards. The samples were extracted three times under 1500 psi pressure at 120 °C. The extracts from each sample were combined and dried on Na₂SO₄. Then, they were concentrated to 5 mL using a rotary evaporator (Model RE52-AA, Shanghai, China), and purified on activated silica-alumina (2:1, v/v) columns. After the cleanup, the samples were then concentrated to 1 mL under a gentle stream of high-purity nitrogen. The concentrated solutions were stored at -20 °C until analysis.

Total 15 PAHs and 9 NPAHs were analyzed using a gas chromatograph/mass spectrometer detector (GC/MSD, Agilent 7890A/5975C) in a selected ion mode (SIM) with a 30 m HP-5 MS capillary column (0.25 mm i.d. × 0.25 μm film thickness). Naphthalene was not included in data analysis, due to the probability of being polluted or evaporated. Prior to the analysis, pyrene-d₁₀ for PAHs and 1-nitropyrene-d₉ for NPAHs was spiked into the solution as internal standards. For the analysis of PAHs, the sample was injected 1 μL in splitless mode at 280 °C, and high purity helium (99.999%) was used as a carrier gas at a stable flow of 1.0 mL/min. The GC temperature was initiated at 60 °C (held for 10 min) and increased to 300 °C at 5 °C min⁻¹, then held for 40 min. The electron impact energy was set at 70 eV with an ion source temperature of 150 °C.

For the analysis of NPAHs, they were analyzed using a GC-MS instrument (Agilent 7890A-5975C, USA) with a negative chemical ionization (NCI) mode using CH₄ as an ionization gas (Bandowe and Meusel, 2017). The GC injection port was held at 240 °C, with an injection volume of 1 μL. The initial temperature of 60 °C was held for 2 min. Then, it was increased to 150 °C at a rate of 45 °C min⁻¹, held for 10 min, and increased to 300 °C at a rate of 5 °C min⁻¹, held for 15 min. The transfer line

temperature was 280 °C. The electron impact energy was set at 70 eV with an ion source and quadrupole temperature of 150 °C. The monitored ion couples for 15 PAHs and 9 NPAHs are listed in Tables S2 and S3.

Standard solutions of 9 NPAHs and 15 PAHs, internal standards (pyrene-d10 for PAHs and 1-nitropyrene-d9 for nitro-PAHs), and surrogate standards (3-nitrofluoranthene-d9 and a mixture of perdeuterated PAHs (naphthalene-d8, acenaphthene-d10, phenanthrene-d10, chrysene-d12, and perylene-d12)) were purchased from AccuStandard, Inc. (New Haven, USA). The 15 PAHs included acenaphthylene (Acy), acenaphthene (Ace), fluorene (Fl), phenanthrene (Phe), anthracene (Ant), fluoranthene (Flt), pyrene (Pyr), benzo[a]anthracene (BaA), chrysene (Chr), benzo[b]fluoranthene (BbF), benzo[k]fluoranthene (BkF), benzo[a]pyrene (BaP), indeno[1,2,3-c,d] pyrene (InP), dibenzo[a,h]anthracene (DBA), and benzo[g,h,i]perylene (BgP). The 9 NPAHs included 2-Nitrobiphenyl (2-NBP), 3-Nitrobiphenyl (3-NBP), 4-Nitrobiphenyl (4-NBP), 3-Nitrophenanthrene (3-NPHE), 2-Nitrofluoranthene (2-NFLT), 3-Nitrofluoranthene (3-NFLT), 1-Nitropyrene (1-NPYR), 7-Nitrobenz(a)anthracene (7-NANT), and 6-Nitrochrysene (6-NCHR). All solvents (methanol, hexane, and dichloromethane) used for sample processing and analyses were HPLC grade purchased from Tedia Co. (USA). Pure water was taken from a Milli-Q water system (Thermo Fisher Scientific Inc., USA). Anhydrous sodium sulfate, silica gel, and alumina were of analytical grade from Sinopharm Chemical Reagent Co. (Shanghai, China). The silica gel (100–200 mesh) and alumina (100–200 mesh) were extracted for 48 h using a Soxhlet apparatus, activated in an oven at 170 and 450 °C for 8 h, and then deactivated with distilled water at a ratio of 5 and 1% (m/m), respectively.

2.4. Quality control and quality assurance

Field blanks were analyzed to evaluate the degree of contamination during the collection and storage of samples. Method blanks (solvents and glass instruments), spiked blanks (standards spiked into solvents), matrix spikes (standards spiked into the sample), and sample duplicates were arranged for quality assurance. PAHs and NPAHs were quantified using internal standard calibration based on five-point calibration curves. The relative deviation of duplicate samples was less than 10%. Recoveries of the surrogate standards are as follows: 75.3–96.9% with acenaphthene-d10, 87.0–106.8% with phenanthrene-d10, 81.2–109.7% with chrysene-d12, $71.2 \pm 110.3\%$ with perylene-d12, and 60.8–118.0% with 1-nitropyrene-d9. The limit of detection (LOD) values for PAHs and NPAHs ranged from 1.2×10^{-3} to 1.1×10^{-2} ng m⁻³ and 4.0×10^{-3} to 1.3×10^{-2} ng m⁻³, respectively.

2.5. Data analysis

Positive matrix factorization (PMF) was applied to quantify the sources of PM_{2.5}-bound PAHs and NPAHs in the YRD region. The used details of the USEPA PMF 5.0 model were described in our previous studies (Liu et al., 2020). Briefly, Eq. (1) illustrates *j* compound species in the *i*th sample as the concentration from *p* independent sources.

$$x_{ij} = \sum_{k=1}^p g_{ik} f_{kj} + e_{ij} \quad (1)$$

where x_{ij} is the *j*th species concentration measured in the *i*th sample, g_{ik} is the species contribution of the *k*th source to the *i*th sample, f_{kj} is the *j*th species fraction from the *k*th source, e_{ij} is the residual for each sample/species, and *p* is the total number of independent sources. Data below the detection limit was retained with the associated uncertainty adjusted. The object function *Q* (Eq. (2)) based on the uncertainties (μ) was used to evaluate the stability of the solution.

$$Q = \sum_{i=1}^n \sum_{j=1}^m \left[\frac{x_{ij} - \sum_{k=1}^p g_{ik} f_{kj}}{\mu_{ij}} \right]^2 \quad (2)$$

According to the Incremental Lifetime Cancer Risk (ILCR) (Zhuo et al., 2017b), human health risks due to inhalation exposure of parent and nitrated PAHs were assessed by the Eq. (3):

$$\text{ILCR} = \text{UR}_{\text{BaP}} \times \text{BaPEQ} = \text{UR}_{\text{BaP}} \times \sum_{i=1}^N (C_i \times \text{TEF}_i) \quad (3)$$

where C_i and TEF_i are the concentration (ng m⁻³) of species *i* and its corresponding Toxic Equivalent Factor (TEF). A unit value of 8.7×10^{-5} (ng m⁻³)⁻¹ was adopted for UR_{BaP} , which is the unit cancer risk factor for BaP (WHO, 2010). TEF values from the literatures (Collins et al., 1998) for priority PAHs and NPAHs are summarized in Table S7.

To gain more insight into the occurrence of PAHs and NPAHs with different pollution levels and their risks resulting from the variations, the PM_{2.5} concentrations were divided into four levels as follows: 0–35 μg m⁻³ (clean), 35–75 μg m⁻³ (light pollution), 75–150 μg m⁻³ (medium pollution) and larger than 150 μg m⁻³ (heavy pollution). Data statistical analysis was processed using SPSS 19.0 (IBM, Armonk, NY, USA). Significance levels of 0.05 and 0.01 were adopted.

3. Results and discussion

3.1. Distribution patterns of PM_{2.5}-bound PAHs and NPAHs

The annual averaged concentrations of total 15 PAHs in NB, NJ and SH were 19.0, 14.3 and 11.0 ng/m³, respectively, while total 9 NPAHs concentrations were 2.24, 1.40 and 1.41 ng/m³ (Tables S3, S4 and S5). Seasonal trends of total PAHs and NPAHs in three cities were similar, with higher concentrations appeared in winter and autumn than those in spring and summer (Fig.1). PM_{2.5} concentrations and Air Quality Index (AQI, estimated by the Ministry of Ecology and Environment of the People's Republic of China, 2012, <http://www.mee.gov.cn>) also shared the same seasonal variation as total PAHs and NPAHs during the sampling periods.

The seasonal pattern of PAHs and NPAHs was predominantly ascribed to the changing of emission sources and meteorological conditions (Khan et al., 2015; Bandowe and Meusel, 2017). Compounds with low molecular weight (LMW), such as PAHs with 2–3 rings were in the vapor phase during summer, while those with high molecular weight (HMW), such as PAHs with 5–6 rings, presented in the particulate phase in the cold time (Albinet et al., 2008; Hu et al., 2019). NPAHs had higher particle-bound fractions than PAHs with the same number of rings, due to their higher MW. Solar radiation was conducive to the transformation of them, while more precipitation and humidity favored the removal of them from the atmosphere. In winter, stable atmospheric structure, low wind speed, high inversion frequency, and low mixing heights would affect the dispersion of PM_{2.5}-bound PAHs and NPAHs (Chen et al., 2020a, 2020b).

Correlation analysis was used to identify the relationship between total PAHs, NPAHs, and other measured parameters (Table 1). For high PM_{2.5} concentrations (PM_{2.5} > 35 μg m⁻³), the concentrations of PAHs and NPAHs showed significantly positive correlations with air pollutants, including SO₂, NO₂, CO, PM₁₀, and PM_{2.5} (*P* < 0.001). These results indicated the contribution of anthropogenic activities on PAHs and NPAHs in the urban area, such as coal combustion and vehicle exhausts. On the clean days (PM_{2.5} < 35 μg m⁻³), the concentrations of PAHs and NPAHs were not correlated with SO₂ and CO. In addition, a negative correlation between NPAH and O₃ was observed. In the YRD, a low concentration of O₃ caused by the weak photochemical reaction was normally observed under the condition of high PM_{2.5} levels (Chen et al., 2020a, 2020b). NPAHs could be formed by heterogeneous photo-oxidation reactions of PAHs with atmospheric oxidants (such as OH, NO₃, and O₃), while photolysis and thermal conversions also affect the occurrence and fate of NPAHs and PAHs (Keyte et al., 2013; Ringuet et al., 2012). Some studies found that high concentrations of PAHs in winter were attributed to the reduced thermal, photolytic and photochemical

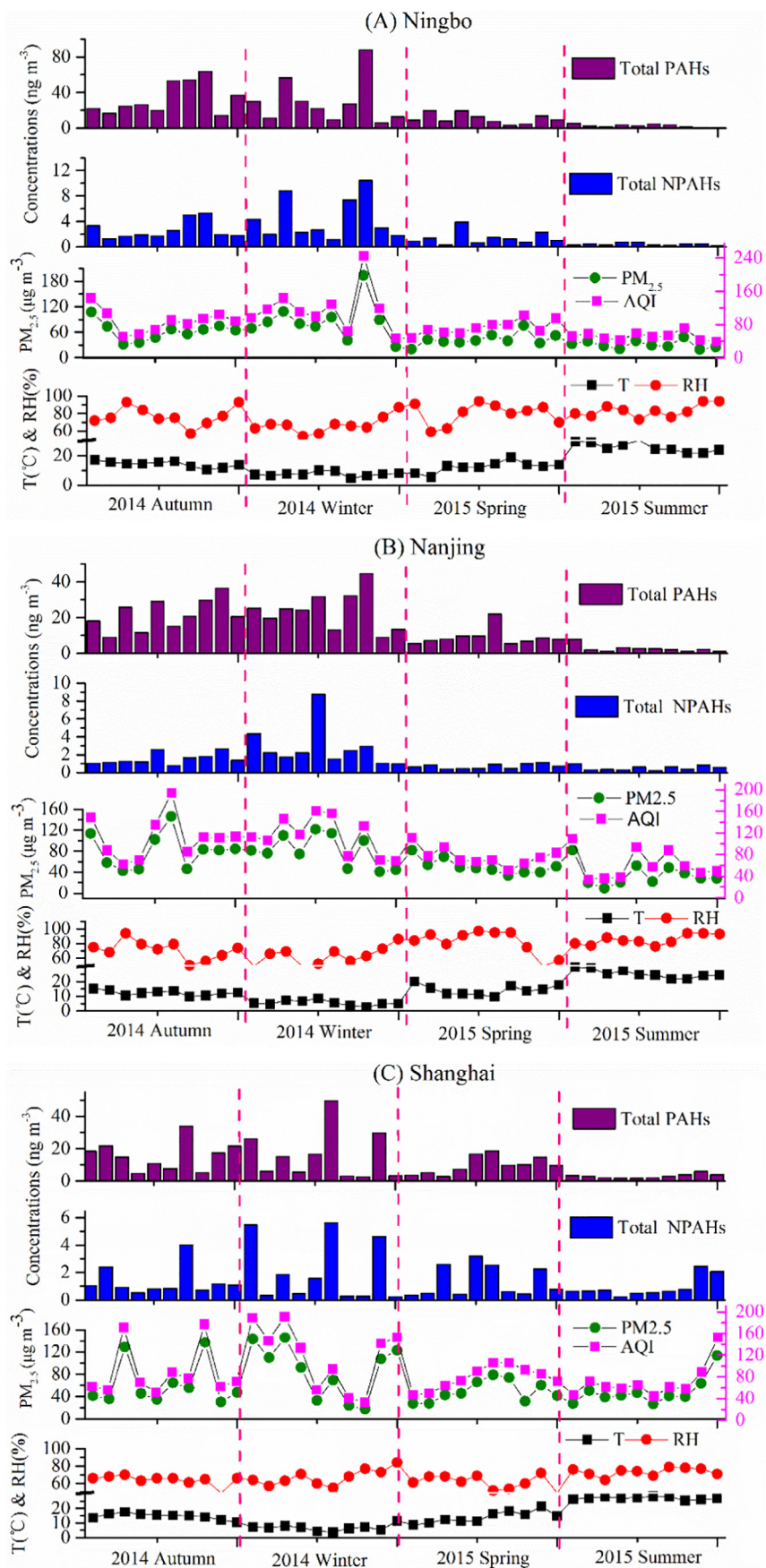


Fig. 1. Seasonal trends of PAHs, Nitro-PAHs, PM_{2.5}, and meteorological factors in the YRD region of China.

Table 1
Correlation coefficients and *P*-values (in parenthesis) between total PAHs and NPAHs and meteorological parameters with different PM_{2.5} level.

	PAHs	NPAHs	AQI	PM _{2.5}	PM ₁₀	SO ₂	CO	NO ₂	O ₃	WS	T	RH
PM _{2.5} < 35 μg m ⁻³												
PAHs	1	0.794**	0.477*	0.516**	0.469*	0.36	-0.083	0.657**	-0.469*	0.111	-0.538**	-0.268
		(<0.001)	(0.010)	(0.005)	(0.012)	(0.060)	(0.674)	(<0.001)	(0.012)	(0.575)	(0.003)	(0.168)
NPAHs		1	0.326	0.397*	0.283	0.291	-0.088	0.548**	-0.394*	-0.089	-0.474*	-0.022
			(0.091)	(0.036)	(0.144)	(0.133)	(0.657)	(0.003)	(0.038)	(0.654)	(0.011)	(0.91)
PM _{2.5} > 35 μg m ⁻³												
PAHs	1	0.784**	0.335**	0.354**	0.438**	0.572**	0.395**	0.492**	-0.472**	-0.280**	-0.489**	-0.277**
		(<0.001)	(0.001)	(0.001)	(<0.001)	(<0.001)	(<0.001)	(<0.001)	(<0.001)	(0.007)	(<0.001)	(0.007)
NPAHs		1	0.389**	0.401**	0.452**	0.558**	0.466**	0.477**	-0.315**	-0.237*	-0.412**	-0.330**
			(<0.001)	(<0.001)	(<0.001)	(<0.001)	(<0.001)	(<0.001)	(0.002)	(0.023)	(<0.001)	(0.001)

*/**Correlation coefficients with an asterisk indicate statistically significant relationships at a = 0.05, and two asterisks mean significant at a = 0.01. Correlation coefficients larger than 0.4 are stated in bold.

degradation of these compounds because of lower temperatures, less radiation and lower levels of atmospheric oxidants (Bandowe and Meusel, 2017; Alves et al., 2017). In contrast, high concentrations of ozone were observed in the afternoon co-varying with solar radiation, to enhance the formation of NPAH from PAH oxidation (Li et al., 2019b).

On the other hand, meteorological parameters had considerable influence on the distribution of PM_{2.5}-bound NPAHs and PAHs. There were significantly negative correlations between NPAHs and PAHs and T (*P* < 0.001), which could be explained by the influence of gas-particle partitioning. More NPAHs and PAHs are expected to partition to the gaseous phase because of the higher ambient temperature. Other studies also found that the relatively low temperature during winter favored the partitioning of NPAHs formed in the gas phase into the aerosol phase (Ma et al., 2016). In addition, PM_{2.5}-bound NPAHs and PAHs have a negative correlation with RH, indicating that there is a greater propensity for wet deposition in high-humidity situations. Especially under high concentrations of PM_{2.5}, a significantly negative correlation (*P* < 0.001) with RH was found. Previous studies have reported that a depositional effect on the particulate matter of semi-volatile polycyclic aromatic compounds because of environmental humidity (Alves et al., 2017). With high concentrations of PM_{2.5}, the concentrations of NPAHs and PAHs presented a negative correlation with wind speed (*P* < 0.05). It revealed that PM_{2.5}-bound NPAHs and PAHs were scavenged by the dilution of air flow under higher wind speed. There were no significant differences between NPAHs, PAHs and wind speed under low PM_{2.5} levels.

As shown in Figs. 2 and S2, the distribution of individual NPAH and different rings PAH in NB, NJ, and SH under different PM_{2.5} levels were analyzed. LMW (3-ring) PAHs are Acy, Ace, Fl, Phe and Ant, medium MW (4-ring) PAHs are FLT, Pyr, BaA and Chr, and the others are HMW (5–6 ring) PAHs. Three cities were dominated by 4–6 ring PAHs, which are mainly low volatile and tend to be adsorbed to particulate matter. With the elevated PM_{2.5} level, the concentrations of 4-ring PAHs and some NPAH such as 3-NBP and 2-FLT increased. For NB, the percentage of 3-NBP ranged from 10% to 50%, and the percentage of 4-ring PAHs increased to 55% (Fig.2). Under the clean (<35 μg m⁻³), light pollution (35–75 μg m⁻³), and medium pollution (75–150 μg m⁻³) conditions, the concentrations of 2-FLT in NJ accounted for 20%, 42% and 48% of the total NPAH, respectively. The percentage of PM_{2.5}-bound 2-NFLT was obviously increased, suggesting the influence of secondary transformation. This is consistent with the fact that a high proportion of secondary components (including sulfate, nitrate and ammonium and secondary organic aerosol) in PM_{2.5} under haze pollution was observed, similar to the finding of other studies (Huang et al., 2014; Wu et al., 2018). In our previous studies, the total percentage of sulfate, nitrate, and ammonium (SNA) in PM_{2.5} in winter was increased to 46.1% in the YRD region, compared to those in spring (Du et al., 2017).

PAHs with different ring numbers can be used to indicate different sources (Hong et al., 2015; Ravindra et al., 2008; Xu et al., 2006).

HMW PAHs are mainly derived from high-temperature combustion processes such as vehicle emissions. The main sources of low and medium MW PAHs are coal, biomass, and natural gas combustion and other lower temperature combustion processes (Ravindra et al., 2008; Xu et al., 2006). In this study, the increase of 4-ring PAHs in three cities indicated the contribution of traffic, coal, and biomass combustion to PM_{2.5} components. The total PAH concentration in Ningbo with a large number of petrochemical industries is much higher than that in Shanghai and Nanjing (Du et al., 2017). Also, which may be related to more effective emission reduction measures in Shanghai and Nanjing, such as the prohibition of yellow labeled heavy-duty vehicles, the development of subways for public transportation, and the use of clean energy in industry, strict and enforced legislation for controlling air pollution (Liu et al., 2018; Yan et al., 2019). The distribution pattern of PM_{2.5}-bound PAHs in these cities was consistent with the PAH emission inventory in China, following the website: <http://inventory.pku.edu.cn/>.

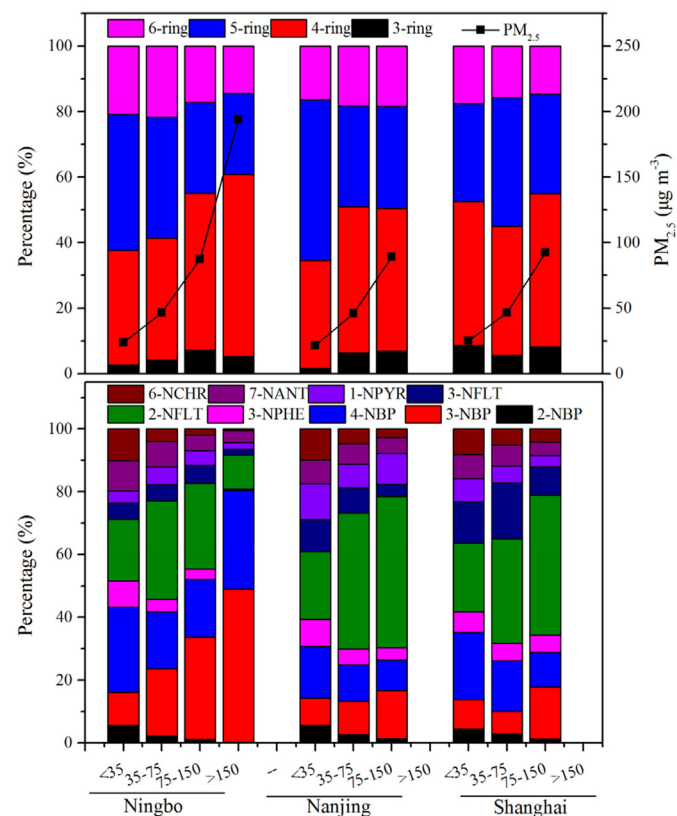


Fig. 2. Percentage of 3–6 rings PAHs and individual NPAH with different PM_{2.5} pollution level.

3.2. Source apportionment of PM_{2.5}-bound PAHs and NPAHs

3.2.1. Isomer ratios analysis

Contributions of anthropogenic activities including vehicles emissions, coal combustion, petroleum and biomass burning to PAHs could be identified qualitatively by isomer ratios such as Ant/(Ant + Phe), BaA/(BaA + Chr), InP/(InP + BgP), and FLT/(FLT + Pyr) (Hong et al., 2015; Zhang et al., 2018). Based on diagnostic ratios and specific molecular markers, sources of PAHs with different PM_{2.5} levels in the YRD region were identified (Fig. S3). The results showed that the FLT/(FLT + Pyr) values were mostly greater than 0.50, indicating the influence of combustion sources. The BaA/(BaA + Chr) > 0.35 implies vehicle emissions, while ratios < 0.35 indicate either petroleum or coal combustion. The Ant/(Ant + Phe) ratio > 0.10 suggested a dominance of combustion sources, while a ratio < 0.10 was an indicator of petroleum. In this study, pyrogenic PAHs including vehicle, oil combustion and natural gas might be an important contributor to PM_{2.5}-bound PAHs in the YRD region. Moreover, the contributions of anthropogenic activities to the distribution of PM_{2.5}-bound PAHs would be changed under different PM_{2.5} levels.

However, it would be difficult to differentiate possible PAH sources only based on diagnostic ratio methods (Tobiszewski and Namiesnik, 2012). Diagnostic ratios of individual PAHs would be changed during the process of atmospheric physics and chemistry from the emission of various sources.

3.2.2. Transformation of NPAH

The atmospheric transformation of PAHs has an important contribution to NPAHs in fine particulates (Bandowe and Meusel, 2017). Previous studies found that 2-NFLT was a predominantly photochemical reaction product, and 1-nitropyrene (1-NPyr) mainly originated from primary emissions (Keyte et al., 2013). The 2-NFLT was generated by the secondary photochemical reaction of the parent FLT with NO₂ under the initiation of NO₃ or OH radicals; thus, the ratio of 2-NFLT to FLT (2-NFLT/FLT) was used to demonstrate the secondary conversion of PAHs in the atmosphere (Lin et al., 2015). As shown in Fig. 3, significant correlations ($R^2 = 0.484$ – 0.657) between the ratios of 2-NFLT/FLT and O₃ were observed. The ratios of 2-NFLT/FLT varied from different seasons in the following order: summer > spring > autumn > winter. The results were attributed to the fact that high temperature and strong solar radiation could enhance the conversion rate from FLT to 2-NFLT

during the warm season. Due to large amounts of FLT originating from human activities, more 2-NFLT via atmospheric secondary formation could still be detected in the cold season.

Photochemical reactions of PAHs with NO₂ and oxidants were found to be an important transformation pathway from PAHs to NPAHs (Lin et al., 2015). The correlation between NPAHs and NO₂ might indicate the predominance of primary sources, including vehicle exhausts and industry. As shown in Fig. S4, PM_{2.5}-bound 2-NFLT was positively correlated with NO₂, suggesting that NO₂ could promote the transformation of PAHs to NPAHs. Much more monitoring data are required for a prediction model to estimate the concentrations of NPAHs based on PAHs and NO₂ data through the established atmospheric chemistry theory.

In addition, the characterization of 6-NCHR/Chr and 1-NP/Pyr during different PM_{2.5} and O₃ pollution levels in three cities were analyzed. The results showed that negative correlation ($R^2 = 0.115$ – 0.238 and $R^2 = 0.072$ – 0.148 , respectively) between the 6-NCHR/Chr and 1-NP/Pyr and PM_{2.5}, while positive correlations ($R^2 = 0.098$ – 0.445 and $R^2 = 0.218$ – 0.518) between the 6-NCHR/Chr and 1-NP/Pyr and O₃. Positive correlations ($R^2 = 0.055$ – 0.149) between the 2-NFLT/1-NPyr and PM_{2.5} in three cities were also found. This result might be related to the process of atmospheric physics and chemistry, especially different sampling periods and places in this study. Current studies have reported that 1-NP/Pyr, 6-NCHR/Chr, 7-NBaA/BaA, and 6-NBaP/BaP were significantly different in emissions from diesel vehicles, coal burning stoves, and wood-burning stoves (Bandowe and Meusel, 2017). These ratios have been suggested to distinguish between locations on the dominant sources of nitro-PAHs. However, the ratios would be changed during the process of atmospheric physics and chemistry from the emission of various sources. Therefore, the mechanism of some nitro-PAH transformed from its parent PAH and some information about the nitro-PAH/PAH ratio from primary emission sources should be further studied.

3.2.3. PMF analysis

PAHs and NPAHs in the atmosphere are mainly emitted from incomplete combustion processes including traffic emission, coal combustion, and biomass burning (Hong et al., 2015; Bandowe and Meusel, 2017). Besides, the secondary formation could be the main source for NPAHs (Lin et al., 2015). In order to quantitatively analyze the sources of PM_{2.5}-bound PAHs and NPAHs in the YRD, the PMF 5.0 model was adopted for four factors (Fig. 4). For factor 1, high levels of FLT, Pyr and Phe were associated with emissions from coal power stations and

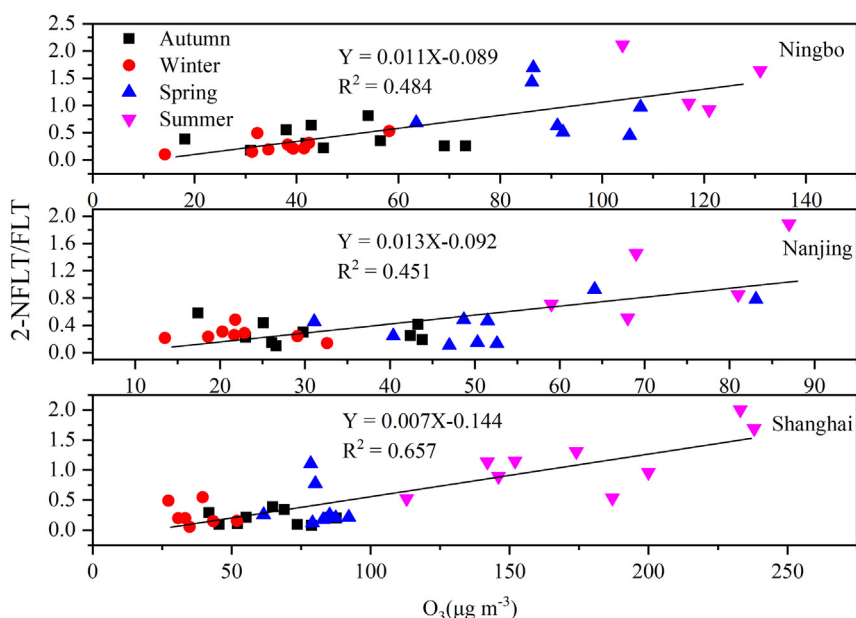


Fig. 3. Linear regression between the 2-NFLT/FLT ratio and O₃ for different seasons.

factories using coal as a fuel (Zhang and Tao, 2008; Soledad Callen et al., 2014). In addition, FLT and Pyr have been used to fingerprint biomass combustion (Jenkins et al., 1996). Previous studies also showed that biomass burning was a significant pollution source for PAHs in the YRD, based on principal component and multivariate linear regression analyses (Li et al., 2020). Therefore, factor 1 can be used as a source profile for coal and biomass combustion. For factor 2, most of NPAHs are the predominant components including 3-NPHE and 2-NFLT. Although NPAHs are produced as direct emissions and through secondary formation, the ratios of 2-NFLT/FLT and 2-NFLT/1-NPyr are typically different from those of primary emissions. For this reason, factor 2 was designated as the secondary formation. For factor 3, the main species are 5–6 ring PAHs, which mainly come from traffic emissions. HMW PAHs, including BkF, BaP, BbF, InP, DBA and BgP, are known to be released into the atmosphere entirely from a vehicle source (He et al., 2008). Some studies have reported that BkF, BaP, BbF, InP and DBA were indicative of gasoline exhaust (Khan et al., 2015). In this study, we also confirmed that these HMW PAHs originated from a traffic source. The factor 4 with high loadings of 2–3 ring PAHs was defined as a mixture of natural gas and volatilization. LMW PAHs (2- and 3-ring), such as Nap, Acy, Ace, Fl, and Ant, are reported to be the main components in the volatilization of crude oil and petroleum products (Yunker et al., 2002). Lighter PAHs were dominant in a natural gas source, and Ant and Fl evaporate from the combustion of natural gas (Khan et al., 2015).

Fig. 5 shows the source analysis results of PAHs and NPAHs in three typical cities of the YRD. The sources of PAHs in $PM_{2.5}$ were mainly traffic emissions, coal and biomass combustion, natural gas, and volatilization, which were consistent with the above results of isomer ratios. Among them, traffic emissions were the most important source of PAHs, and their contributions to total PAHs in SH, NJ and NB were 44.9%, 47.6% and 48.7% respectively. The second-largest source was coal and biomass combustion, contributing 27.6%, 31.8%, and 36.0% in SH, NJ, and NB, respectively, and natural gas and volatilization accounted for 27.5%, 20.6%, and 15.3% of the sources of PAHs.

As discussed above, the secondary formation could be an important factor for the elevated level of some NPAHs such as 2-NFLT. The relative contributions of four sources in different cities were compared. As shown in Fig. 5, the secondary formation was the dominant source and thus contributed 39.8–53.8% of the total NPAH concentrations. The proportions in SH, NB and NJ were 53.8%, 39.8%, and 46.8%

respectively. Traffic emissions were also an important source of NPAHs in $PM_{2.5}$, accounting for 10.9%–24.7%. Natural gas and volatilization (15.4–19.4%) and coal and biomass combustion (15.9–19.6%) were the other sources of NPAHs. This is consistent with the common crop burning activities and the energy consumption pattern in the YRD region (Chen et al., 2017).

3.2.4. Backward trajectory analysis

Overall, regional transport had important effects on the source contributions of $PM_{2.5}$, PAHs, and NPAHs in the YRD. Backward trajectory analysis during the monitoring period was performed to explore the transport pathway of the air masses using the Hybrid Single Particle Lagrangian Integrated Trajectory model (HYSPPLIT). The 72-h backward trajectory analysis was conducted at a ground elevation of 500 m at the monitoring sites. The occurrences of each cluster for different $PM_{2.5}$ concentrations were illustrated in Fig. S5. For the lowest $PM_{2.5}$ concentrations ($<35 \mu\text{g m}^{-3}$), three monitoring sites were mainly affected by air masses from the ocean, bringing clean air from the East Sea and the Yellow Sea to the studied region. For the light pollution level ($35 \mu\text{g m}^{-3} < PM_{2.5} < 75 \mu\text{g m}^{-3}$), air masses originated predominantly from the Shandong peninsula and the YRD region. The highest $PM_{2.5}$ concentrations ($>75 \mu\text{g m}^{-3}$) were observed when the air masses originated from Siberia and North China through long-range transport. Similar air masses were found for the top 50% of high PAHs and NPAHs concentrations in the YRD (Figs. S6 and S7). The air mass transported from North China to the YRD region caused the elevated concentration of $PM_{2.5}$ -bound PAHs and NPAHs in the atmosphere.

3.3. Human health risks of $PM_{2.5}$ -bound PAHs and NPAHs

Based on the various pollution level, the mean BaP equivalent concentrations of PAHs and NPAHs, and their contributions to the total carcinogenic activity in different cities were calculated (Table S7). Under the pollution level ($PM_{2.5} > 35 \mu\text{g m}^{-3}$), total BaP equivalent values of PAHs ranged from 1.78 to 15.35 ng m^{-3} , exceeding the newest limited value (1.0 ng m^{-3}) in the Ambient Air Quality Standard of China. BaP equivalent concentrations in North China could exceed the national limited value by 2–10 times (Zhuo et al., 2017a, 2017b). As shown in Table S7, HMW PAHs including BaA, BbF, BaP, DBA showed larger TEQ than LMW PAHs. And, the most dominant compound was BaP, approximately contributing to more than 50% of the total HMW PAHs. The BaP

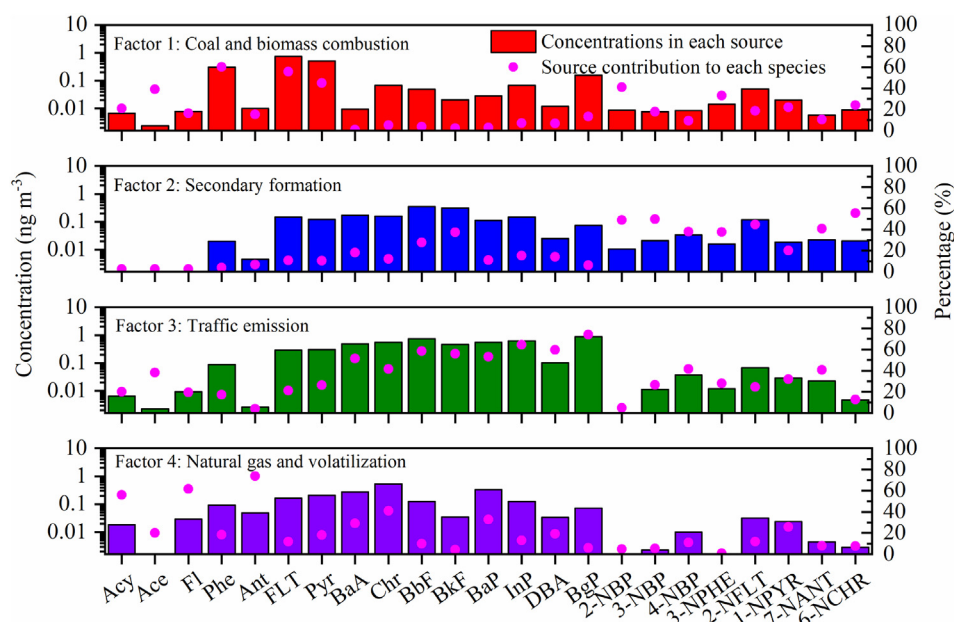


Fig. 4. Source profiles and relative contribution of each source to the target species based on the PMF analysis.

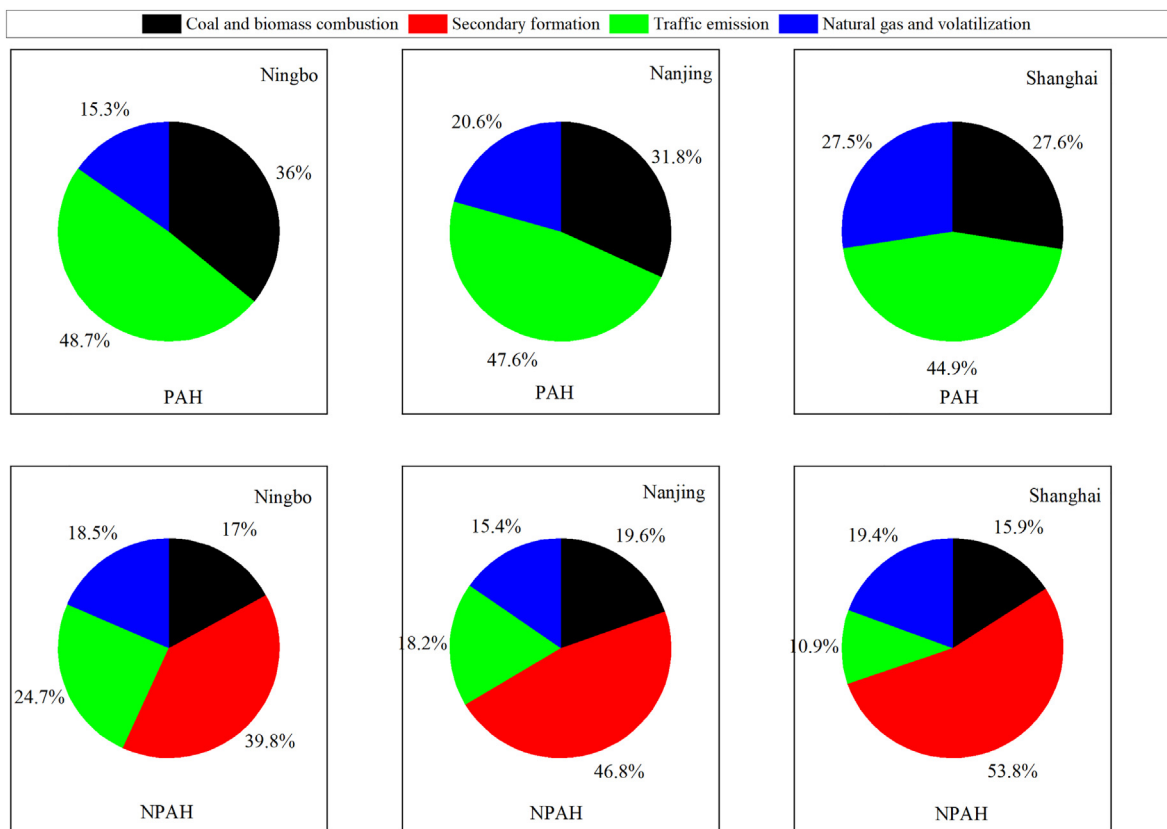


Fig. 5. Source contributions for PM_{2.5}-bound PAHs and NPAHs in the YRD region of China.

equivalent values of total PAHs increased with the increase of the concentrations of PM_{2.5} (Fig. 6), suggesting the potential risks of particulate PAH to human health during haze pollution events. As shown in Fig. 6, on the clean days, BaP equivalent concentrations for a different type of PAHs and individual NPAHs was defined as 1. For different PM_{2.5} pollution levels, BaP equivalent concentrations of PAHs with different ring numbers were 10–25 times higher than those in the clean days (Fig. 6). In contrast, BaP equivalent values of total NPAH were not obviously influenced by the pollution level (Table S7). Based on the limited TEFs of NPAHs, overall BaP equivalent toxicities were not evaluated. For

different types of NPAHs, the BaP equivalent concentration of 2-NFLT during the heavy pollution days was six times higher than that in the clean days (Fig. 6).

Except for the clean days, the ILCRs due to 15 PAHs inhalation exposure were higher than the level of 1.0×10^{-4} , indicating high risks of lung cancer among the population in the YRD region (Fig. 7). Health risks of PM_{2.5}-bound PAHs in three cities all increased as the pollution level increased. The calculated average ILCRs due to inhalation exposure to PAHs in Ningbo and Nanjing were higher than that in Shanghai. For future risk assessment, other PAH derivatives should be taken into account (Zhuo et al., 2017a, 2017b).

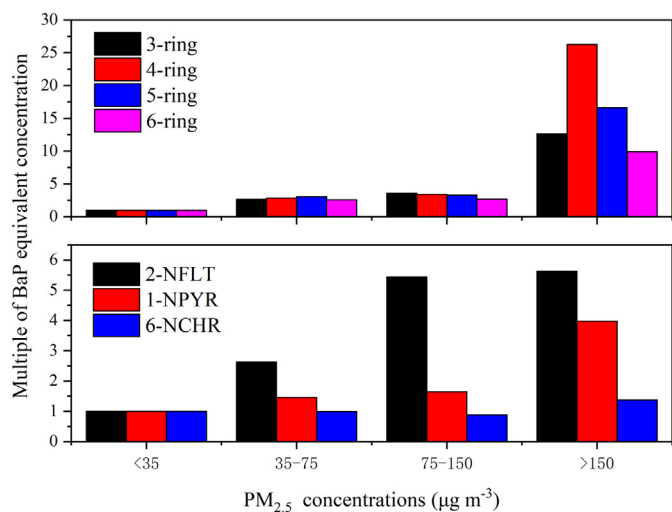


Fig. 6. Multiple of BaP equivalent concentration for different PAH and NPAH with different PM_{2.5} pollution level, compare to the clean day.

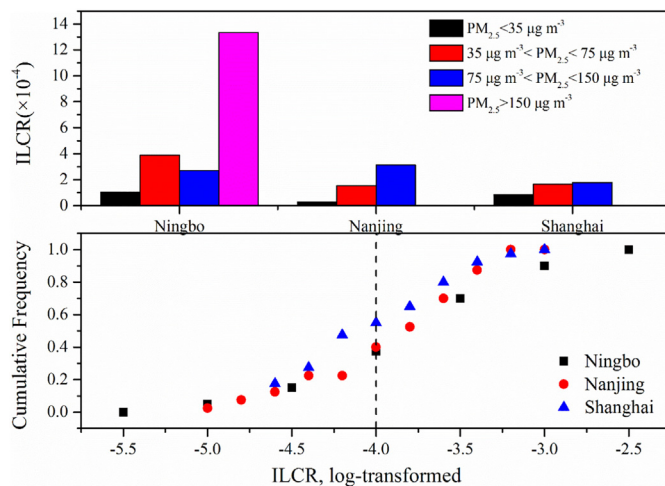


Fig. 7. The incremental lifetime cancer risk (ILCR) due to inhalation exposure of total PAHs with different PM_{2.5} level in the YRD region.

4. Conclusions

The seasonal pattern of PM_{2.5}-bound PAHs and NPAHs in the YRD were predominantly ascribed to the changing of emission sources and meteorological conditions. PAHs and NPAHs showed significantly positive correlations with criteria air pollutants, indicating the influence of anthropogenic activities. PM_{2.5}-bound 2-NFLT was positively correlated with O₃ and NO₂, suggesting that anthropogenic emissions could promote the transformation of PAHs to NPAHs during the warm season. Moreover, the PM_{2.5} level might change the contributions of anthropogenic activities to the distribution of PM_{2.5}-bound PAHs. Based on PMF analysis, traffic emissions, coal and biomass combustion, and natural gas and volatilization were the major sources of PAHs, and secondary formation had the predominant contribution to total NPAH concentrations. Backward trajectory analysis showed that the air mass originating from North China to the YRD region could cause the increase of PM_{2.5}-bound PAHs and NPAHs concentrations.

With the elevated PM_{2.5} level, the percentage of 4-ring PAHs and typical NPAHs including 3-NBP and 2-NFLT increased by 19–40%, and health risks of PAHs and NPAHs were correspondingly enhanced. Compare to the clean days, BaP equivalent concentrations of total PAHs and NPAHs during haze pollution days were enhanced by 10–25 and 2–6 times, respectively. The Incremental Lifetime Cancer Risks (ILCRs) of the 16 EPA priority PAHs by inhalation exposure also indicated potential human health risks in the YRD region. The results implied that health risks of PM_{2.5}-bound PAHs and NPAHs could be sharply enhanced with the increase of PM_{2.5} pollution level, and effective emission control measures should be considered for air pollution forecast.

CRedit authorship contribution statement

Youwei Hong: Conceptualization, Methodology, Formal analysis, Writing – original draft. **Xinbei Xu:** Investigation, Formal analysis, Writing – original draft, Data curation. **Dan Liao:** Investigation, Formal analysis, Writing – original draft, Data curation. **Xiaoting Ji:** Investigation, Formal analysis, Writing – original draft, Data curation. **Zhenyu Hong:** Methodology, Resources, Investigation. **Yanting Chen:** Project administration, Visualization. **Lingling Xu:** Software, Validation. **Mengren Li:** Software, Validation. **Hong Wang:** Project administration, Visualization. **Han Zhang:** Methodology, Resources, Investigation. **Hang Xiao:** Writing – review & editing. **Sung-Deuk Choi:** Writing – review & editing. **Jinsheng Chen:** Funding acquisition, Writing – review & editing.

Declaration of competing interest

The authors declare that they have no known competing financial interests or personal relationships that could have appeared to influence the work reported in this paper.

Acknowledgments

This research was financially supported by the National Key Research and Development Program (2016YFC0112200), the FJIRSM&IUE Joint Research Fund (RHZX-2019-006), State Key Laboratory of Environmental Chemistry and Ecotoxicology, Research Center for Eco-Environmental Sciences, CAS (KF2020-06), Center for Excellence in Regional Atmospheric Environment project (EOL1B20201), the Xiamen Youth Innovation Fund Project (3502220206094) and the Foreign Cooperation Project of Fujian Province (2020I0038).

Appendix A. Supplementary data

Supplementary data to this article can be found online at <https://doi.org/10.1016/j.scitotenv.2021.145402>.

References

- Albinet, A., Leoz-Garziandia, E., Budzinski, H., Villenave, E., Jaffrezou, J.L., 2008. Nitrated and oxygenated derivatives of polycyclic aromatic hydrocarbons in the ambient air of two French alpine valleys – part 1: concentrations, sources and gas/particle partitioning. *Atmos. Environ.* 42, 43–54.
- Alves CA, Vicente AM, Custodio D, Cerqueira M, Nunes T, Pio C, et al. Polycyclic aromatic hydrocarbons and their derivatives (nitro-PAHs, oxygenated PAHs, and azaarenes) in PM_{2.5} from Southern European cities. *Sci. Total Environ.* 2017; 595: 494–504.
- Bandowe, B.A.M., Meusel, H., 2017. Nitrated polycyclic aromatic hydrocarbons (nitro-PAHs) in the environment – a review. *Sci. Total Environ.* 581, 237–257.
- Chen, J., Li, C., Ristovski, Z., Milic, A., Gu, Y., Islam, M.S., Wang, S., Hao, J., Zhang, H., He, C., Guo, H., Fu, H., Miljevic, B., Morawska, L., Phong, T., Fat, Y.L.A.M., Pereira, G., Ding, A., Huang, X., Dumka, U.C., 2017. A review of biomass burning: emissions and impacts on air quality, health and climate in China. *Sci. Total Environ.* 579, 1000–1034.
- Chen, Z., Chen, D., Zhao, C., Kwan, M.-P., Cai, J., Zhuang, Y., Zhao, B., Wang, X., Chen, B., Yang, J., Li, R., He, B., Gao, B., Wang, K., Xu, B., 2020a. Influence of meteorological conditions on PM_{2.5} concentrations across China: a review of methodology and mechanism. *Environ. Int.* 139.
- Chen, L., Zhu, J., Liao, H., Yang, Y., Yue, X., 2020b. Meteorological influences on PM_{2.5} and O₃ trends and associated health burden since China's clean air actions. *Sci. Total Environ.* 744.
- Cheng, Z., Luo, L.; Wang, S.X.; Wang, Y.G.; Sharma, S.; Shimadera, H.; Wang, X.L.; Bressi, M.; de Miranda, R.M.; Jiang, J.K.; Zhou, W.; Fajardo, O.; Yan, N.Q.; Hao, J.M. Status and characteristics of ambient PM_{2.5} pollution in global megacities. *Environment International* 2016;89–90:212–221.
- Cohen, A.J.; Brauer, M.; Burnett, R.; Anderson, H.R.; Frostad, J.; Estep, K.; Balakrishnan, K.; Brunekreef, B.; Dandona, L.; Dandona, R.; Feigin, V.; Freedman, G.; Hubbell, B.; Jobling, A.; Kan, H.; Knibbs, L.; Liu, Y.; Martin, R.; Morawska, L.; Pope, C.A., III; Shin, H.; Straif, K.; Shaddick, G.; Thomas, M.; van Dingenen, R.; van Donkelaar, A.; Vos, T.; Murray, C.J.L.; Forouzanfar, M.H. Estimates and 25-year trends of the global burden of disease attributable to ambient air pollution: an analysis of data from the Global Burden of Diseases Study 2015. *Lancet* 2017;389:1907–1918.
- Collins, J.F., Brown, J.P., Alexeeff, G.V., Salmon, A.G., 1998. Potency equivalency factors for some polycyclic aromatic hydrocarbons and polycyclic aromatic hydrocarbon derivatives. *Regulatory Toxicology Pharmacology* 28, 45–54.
- Du, W., Zhang, Y., Chen, Y., Xu, L., Chen, J., Deng, J., et al., 2017. Chemical characterization and source apportionment of PM_{2.5} during spring and winter in the Yangtze River Delta, China. *Aerosol Air Qual. Res.* 17, 2165–2180.
- Guan, W., Zheng, X., Chung, K., Zhong, N., 2016. Impact of air pollution on the burden of chronic respiratory diseases in China: time for urgent action. *Lancet* 388, 1939–1951.
- He, L., Hu, M., Zhang, Y., Huang, X., Yao, T., 2008. Fine particle emissions from on-road vehicles in the Zhujiang tunnel. *China. Environmental Science & Technology* 42, 4461–4466.
- He, J., Fan, S., Meng, Q., Sun, Y., Zhang, J., Zu, F., 2014. Polycyclic aromatic hydrocarbons (PAHs) associated with fine particulate matters in Nanjing, China: distributions, sources and meteorological influences. *Atmos. Environ.* 89, 207–215.
- Hong, Y., Chen, J., Zhang, F., Zhang, H., Xu, L., Yin, L., Chen, Y., 2015. Effects of urbanization on gaseous and particulate polycyclic aromatic hydrocarbons and polychlorinated biphenyls in a coastal city, China: levels, sources, and health risks. *Environ. Sci. Pollut. Res.* 22, 14919–14931.
- Hu, H., Tian, M., Zhang, L., Yang, F., Peng, C., Chen, Y., Shi, G., Yao, X., Jiang, C., Wang, J., 2019. Sources and gas-particle partitioning of atmospheric parent, oxygenated, and nitrated polycyclic aromatic hydrocarbons in a humid city in southwest China. *Atmos. Environ.* 206, 1–10.
- Huang, R., Zhang, Y., Bozzetti, C., Ho, K., Cao, J., Han, Y., Daellenbach, K.R., Slowik, J.G., Platt, S.M., Canonaco, F., Zotter, P., Wolf, R., Pieber, S.M., Brun, E.A., Crippa, M., Ciarelli, G., Piazzalunga, A., Schwikowski, M., Abbaszade, G., Schnelle-Kreis, J., Zimmermann, R., An, Z., Szidat, S., Baltensperger, U., El Haddad, I., Prevot, A.S.H., 2014. High secondary aerosol contribution to particulate pollution during haze events in China. *Nature* 514, 218–222.
- Idowu, O., Semple, K.T., Ramadass, K., O'Connor, W., Hansbro, P., Thavamani, P., 2019. Beyond the obvious: environmental health implications of polar polycyclic aromatic hydrocarbons. *Environ. Int.* 123, 543–557.
- Jenkins, B.M., Jones, A.D., Turn, S.Q., Williams, R.B., 1996. Emission factors for polycyclic aromatic hydrocarbons from biomass burning. *Environmental Science & Technology* 30 (8), 2462–2469.
- Keyte, I.J., Harrison, R.M., Lammel, G., 2013. Chemical reactivity and long-range transport potential of polycyclic aromatic hydrocarbons – a review. *Chem. Soc. Rev.* 42, 9333–9391.
- Khan, M.F., Latif, M.T., Lim, C.H., Amil, N., Jaafar, S.A., Dominick, D., et al., 2015. Seasonal effect and source apportionment of polycyclic aromatic hydrocarbons in PM_{2.5}. *Atmos. Environ.* 106, 178–190.
- Li, J., Liao, H., Hu, J., Li, N., 2019a. Severe particulate pollution days in China during 2013–2018 and the associated typical weather patterns in Beijing-Tianjin-Hebei and the Yangtze River Delta regions. *Environ. Pollut.* 248, 74–81.
- Li, J., Yang, L., Gao, Y., Jiang, P., Li, Y., Zhao, T., Zhang, J., Wang, W., 2019b. Seasonal variations of NPAHs and OPAHs in PM_{2.5} at heavily polluted urban and suburban sites in North China: concentrations, molecular compositions, cancer risk assessments and sources. *Ecotoxicol. Environ. Saf.* 178, 58–65.
- Li, B., Zhou, S., Wang, T., Zhou, Y., Ge, L., Liao, H., 2020. Spatio-temporal distribution and influencing factors of atmospheric polycyclic aromatic hydrocarbons in the Yangtze River Delta. *J. Clean. Prod.* 267.
- Lin, Y., Ma, Y., Qiu, X., Li, R., Fang, Y., Wang, J., Zhu, Y., Hu, D., 2015. Sources, transformation, and health implications of PAHs and their nitrated, hydroxylated, and oxygenated derivatives in PM_{2.5} in Beijing. *J. Geophys. Res.-Atmos.* 120, 7219–7228.

- Lin, Y., Chou, F., Li, Y., Jhang, S., Shangdiar, S., 2019. Effect of air pollutants and toxic emissions from various mileage of motorcycles and aerosol related carcinogenicity and mutagenicity assessment. *J. Hazard. Mater.* 365, 771–777.
- Liu, Y., Yu, Y., Liu, M., Lu, M., Ge, R., Li, S., et al., 2018. Characterization and source identification of PM_{2.5}-bound polycyclic aromatic hydrocarbons (PAHs) in different seasons from Shanghai, China. *Sci. Total Environ.* 644, 725–735.
- Liu, T., Hu, B., Yang, Y., Li, M., Hong, Y., Xu, X., Xu, L., Chen, N., Chen, Y., Xiao, H., Chen, J., 2020. Characteristics and source apportionment of PM_{2.5} on an island in Southeast China: impact of sea-salt and monsoon. *Atmos. Res.* 235.
- Ma, Y., Cheng, Y., Qiu, X., Lin, Y., Cao, J., Hu, D., 2016. A quantitative assessment of source contributions to fine particulate matter (PM_{2.5})-bound polycyclic aromatic hydrocarbons (PAHs) and their nitrated and hydroxylated derivatives in Hong Kong. *Environ. Pollut.* 219, 742–749.
- Ma, L., Li, B., Liu, Y., Sun, X., Fu, D., Sun, S., Thapa, S., Geng, J., Qi, H., Zhang, A., Tian, C., 2020. Characterization, sources and risk assessment of PM_{2.5}-bound polycyclic aromatic hydrocarbons (PAHs) and nitrated PAHs (NPAHs) in Harbin, a cold city in Northern China. *Journal of Clean Production* 264.
- Ministry of Ecology and Environment of the People's Republic of China, "Technical Regulation on Ambient Air Quality Index (in Chinese), HJ 633-2012, Ministry of Ecology and Environment of the People's Republic of China, Beijing, 2012. http://www.mee.gov.cn/ywggz/fgbz/bzwbw/jcfbz/201203/t20120302_224166.shtml.
- Oliveira, M., Slezakova, K., Delerue-Matos, C., Pereira, M.C., Morais, S., 2019. Children environmental exposure to particulate matter and polycyclic aromatic hydrocarbons and biomonitoring in school environments: a review on indoor and outdoor exposure levels, major sources and health impacts. *Environ. Int.* 124, 180–204.
- Ravindra, K., Sokhi, R., Van Grieken, R., 2008. Atmospheric polycyclic aromatic hydrocarbons: source attribution, emission factors and regulation. *Atmos. Environ.* 42, 2895–2921.
- Ringuet, J., Albinet, A., Leoz-Garziandia, E., Budzinski, H., Villenave, E., 2012. Diurnal/nocturnal concentrations and sources of particulate-bound PAHs, OPAHs and NPAHs at traffic and suburban sites in the region of Paris (France). *Sci. Total Environ.* 437, 297–305.
- Soledad Callen, M., Iturmendi, A., Manuel, Lopez J., 2014. Source apportionment of atmospheric PM_{2.5}-bound polycyclic aromatic hydrocarbons by a PMF receptor model. Assessment of potential risk for human health. *Environ. Pollut.* 195, 167–177.
- Tobiszewski, M., Namiesnik, J., 2012. PAH diagnostic ratios for the identification of pollution emission sources. *Environ. Pollut.* 162, 110–119.
- Tomaz, S., Shahpoury, P., Jaffrezo, J.-L., Lamme, G., Perraudin, E., Villenave, E., Albinet, A., 2016. One-year study of polycyclic aromatic compounds at an urban site in Grenoble (France): seasonal variations, gas/particle partitioning and cancer risk estimation. *Sci. Total Environ.* 565, 1071–1083.
- Wang, Q., Liu, M., Yu, Y., Li, Y., 2016. Characterization and source apportionment of PM_{2.5}-bound polycyclic aromatic hydrocarbons from Shanghai city, China. *Environ. Pollut.* 218, 118–128.
- Wei, C., Han, Y., Bandowe, B.A.M., Cao, J., Huang, R., Ni, H., Tian, J., Wilcke, W., 2015. Occurrence, gas/particle partitioning and carcinogenic risk of polycyclic aromatic hydrocarbons and their oxygen and nitrogen containing derivatives in Xi'an, central China. *Sci. Total Environ.* 505, 814–822.
- World Health Organization (WHO), 2010. WHO Guidelines for Indoor Air Quality: Selected Pollutants. WHO Regional office for Europe, Denmark.
- Wu, X., Vu, T.V., Shi, Z., Harrison, R.M., Liu, D., Cen, K., 2018. Characterization and source apportionment of carbonaceous PM_{2.5} particles in China - a review. *Atmos. Environ.* 189, 187–212.
- Xie, J.W., Jin, L., He, T.T., Chen, B.W., Luo, X.S., Feng, B.H., et al., 2019. Bacteria and antibiotic resistance genes (ARGs) in PM_{2.5} from China: implications for human exposure. *Environmental Science & Technology* 53, 963–972.
- Xu, S.S., Liu, W.X., Tao, S., 2006. Emission of polycyclic aromatic hydrocarbons in China. *Environmental Science & Technology* 40, 702–708.
- Yan, D., Wu, S., Zhou, S., Tong, G., Li, F., Wang, Y., et al., 2019. Characteristics, sources and health risk assessment of airborne particulate PAHs in Chinese cities: a review. *Environ. Pollut.* 248, 804–814.
- Yang, L., Wang, W., Lung, S., Sun, Z., Chen, C., Chen, J., Zou, Q., Lin, Y., Lin, C., 2017. Polycyclic aromatic hydrocarbons are associated with increased risk of chronic obstructive pulmonary disease during haze events in China. *Sci. Total Environ.* 574, 1649–1658.
- Yin, P.; Brauer, M.; Cohen, A.J.; Wang, H.; Li, J.; Burnett, R.T.; Stanaway, J.D.; Causey, K.; Larson, S.; Godwin, W.; Frostad, J.; Marks, A.; Wang, L.; Zhou, M.; Murray, C.J.L. The effect of air pollution on deaths, disease burden, and life expectancy across China and its provinces, 1990–2017: an analysis for the Global Burden of Disease Study 2017. *The Lancet Planetary health* 2020.
- Yunker, M.B., Macdonald, R.W., Vingarzan, R., Mitchell, R.H., Goyette, D., Sylvestre, S., 2002. PAHs in the Fraser River basin: a critical appraisal of PAH ratios as indicators of PAH source and composition. *Org. Geochem.* 33 (4), 489–515.
- Zhang, Y., Tao, S., 2008. Seasonal variation of polycyclic aromatic hydrocarbons (PAHs) emissions in China. *Environ. Pollut.* 156, 657–663.
- Zhang, J., Yang, L., Mellouki, A., Chen, J., Chen, X., Gao, Y., Jiang, P., Li, Y., Yu, H., Wang, W., 2018. Diurnal concentrations, sources, and cancer risk assessments of PM_{2.5}-bound PAHs, NPAHs, and OPAHs in urban, marine and mountain environments. *Chemosphere* 209, 147–155.
- Zhang, L., Morisaki, H., Wei, Y., Li, Z., Yang, L., Zhou, Q., Zhang, X., Xing, W., Hu, M., Shima, M., Toriba, A., Hayakawa, K., Tang, N., 2020. PM_{2.5}-bound polycyclic aromatic hydrocarbons and nitro-polycyclic aromatic hydrocarbons inside and outside a primary school classroom in Beijing: concentration, composition, and inhalation cancer risk. *Sci. Total Environ.* 705.
- Zhuo, S., Du, W., Shen, G., Wang, R., Pan, X., Li, T., Han, Y., Li, Y., Pan, B., Peng, X., Cheng, H., Wang, X., Shi, G., Xing, B., Tao, S., 2017a. Urban air pollution and health risks of parent and nitrated polycyclic aromatic hydrocarbons in two megacities, southwest China. *Atmos. Environ.* 166, 441–453.
- Zhuo, S., Shen, G., Zhu, Y., Du, W., Pan, X., Li, T., Han, Y., Li, B., Liu, J.F., Cheng, H., Xing, B., Tao, S., 2017b. Source-oriented risk assessment of inhalation exposure to ambient polycyclic aromatic hydrocarbons and contributions of non-priority isomers in urban Nanjing, a megacity located in Yangtze River Delta, China. *Environmental Pollution* 224, 796–809.